The Journal of Veterinary Medical Science

FULL PAPER

Pharmacology

Effects of omega-7 palmitoleic acids on skeletal muscle differentiation in a hyperglycemic condition

Yayoi TOKUNAGA[1)], Hitomi YOSHIZAKI[2)], Akiyo TORIUMI[3)], Ritsuko KAWAHARADA[4)], Chisato ISHIDA[5)], Masatoshi HORI[1)]* and Akio NAKAMURA[2)]*

[1)]Graduate School of Agriculture and Life Sciences, Faculty of Agriculture, The University of Tokyo, 1-1-1 Yayoi, Bunkyo-ku, Tokyo 113-8657, Japan

[2)]Department of Molecular Nutrition, Faculty of Human Life Sciences, Jissen Women's University, 4-1-1 Osakaue, Hino, Tokyo 191-8510, Japan

[3)]Graduate School of Medical and Dental Sciences, Comprehensive Reproductive Medicine, National University Corporation Tokyo Medical and Dental University, 1-5-45 Yushima, Bunkyo-ku, Tokyo 113-8510, Japan

[4)]Department of Health and Nutrition, Takasaki University of Health and Welfare, 37-1 Nakaorui-machi, Takasaki, Gunma 370-0033, Japan

[5)]Department of Nutrition, Japanese Haramachi Red Cross Hospital, 698 Haramachi, Agatsumagun, Higashiagatsuma-machi, Gunma 377-0801, Japan

ABSTRACT. Maternal obesity and diabetes are known to be involved in fetal myogenesis, but the later stages of myogenesis are not well understood. In this study, we investigated the influence of a hyperglycemic environment on L6 skeletal myoblast differentiation and the function of omega-7 palmitoleic acids. Exposure to a high concentration of glucose (25 mM) in high-glucose culture medium (HG) increased the expression of myogenic genes (*MyoD*, *Myogenin*, *MRF4*, *Myhc2x*, and *Myhc2a*) and the synthesis of myosin. HG also activated the PI3K/AKT pathway revealed muscle cell differentiation. Furthermore, the levels of reactive oxygen species (ROS) and an inflammatory cytokine (*Tnfaip3*; tumor necrosis factor alpha-induced protein 3), which are crucial for the growth and differentiation of skeletal muscle, were increased by HG. Palmitoleic acids suppressed the expression levels of myogenic regulatory genes and increased the expression level of a cell proliferation-related gene (*Pax3*). Trans-palmitoleic acid and eicosapentaenoic acid (TPA and EPA) increased the phosphorylation level of MAPK/ERK1/2 and downregulated ROS generation and *Tnfaip3* expression. In contrast, cis-palmitoleic acid inactivated MAPK/ERK1/2, leading to increased ROS generation. In conclusion, a hyperglycemic environment mediated by HG induced excessive muscle differentiation. Palmitoleic acids inhibited myoblast differentiation by downregulating muscle-specific genes. Moreover, trans-palmitoleic acids may have beneficial antioxidant and/or anti-inflammatory effects in cells.

KEY WORDS: differentiation, fatty acid, skeletal muscle

J. Vet. Med. Sci.
83(9): 1369–1377, 2021
doi: 10.1292/jvms.21-0309

Received: 31 May 2021
Accepted: 29 June 2021
Advanced Epub:
12 July 2021

The prevalence of maternal obesity and diabetes is increasing with the increasing age of primiparas. It has been suggested that such obesity and diabetes may cause complications, such as developmental disorders and macrosomia [2, 10]. During pregnancy, the energy metabolism status of the mother changes significantly [3, 8, 22]: lipogenesis is promoted in the early stages of pregnancy, and in the later stages of pregnancy, insulin resistance increases due to increased levels of maternal free fatty acids [3]. In addition, maternal obesity and diabetes further increase the insulin resistance [3], leading to a hyperglycemic intrauterine environment, which is associated with a high risk of macrosomia [34]. Furthermore, it has been reported that children born from an intrauterine hyperglycemic environment are more likely to develop metabolic syndrome and obesity in the future [5].

Skeletal muscle is an essential organ for energy metabolism. It has been reported that suboptimal fetal programming of skeletal muscle development increases lipogenesis and fibrosis in skeletal muscle, and further weakens insulin signals [32]. However, it is not known how the hyperglycemic environment, which is an abnormal state, affects the development and differentiation of skeletal muscle cells that exist from the early stage of fetal development, including during cell proliferation, differentiation, and transformation into organs. It is necessary to examine this by using a cell model.

Dietary supplements that are often taken during pregnancy include n-3 polyunsaturated fatty acids, such as eicosapentaenoic

*Correspondence to: Hori, M.: horimasa@g.ecc.u-tokyo.ac.jp, Nakamura, A.: nakamura-akio@jissen.ac.jp

acid (EPA). EPA is expected to improve fat-induced insulin resistance and some metabolic disorders [15, 25]. It has been reported that EPA has effects on normal fetal growth, such as effects on the cell membrane composition and brain development [12]. Furthermore, it is thought that EPA suppresses the generation of reactive oxygen species (ROS) and inflammation caused by the increased metabolism of the mother during pregnancy [14, 21]. However, long-term EPA intake can cause bleeding in the mother during childbirth [31]. Palmitoleic acids are also expected to be useful as antioxidant nutrients in prenatal or perinatal dietary supplements [30]. Moreover, a previous study on the relationship between palmitoleic acids and diabetes as well as insulin resistance showed that trans-palmitoleic acid (TPA) significantly decreased the risk of diabetes [20]. The effect is reported about bioactivity of the palmitoleic acids in this way, but is not reported in two isomeric functions. The aim of the present study was to investigate the influence of a hyperglycemic environment on L6 skeletal myoblast differentiation and the function of omega-7 palmitoleic acids.

MATERIALS AND METHODS

Reagents and chemicals

EPA (C20:5, ω-3) was purchased from Tokyo Chemical Industry Co., Ltd. (Tokyo, Japan). Cis-palmitoleic acid (cis-C16:1, ω-7; CPA) and bovine serum albumin (BSA) were purchased from Sigma-Aldrich (St. Louis, MO, USA). Trans-Palmitoleic acid (trans-C16:1, ω-7; TPA) was purchased from Cayman Chemical Co. (Ann Arbor, MI, USA). All other reagents were of commercially analytical and extra-pure grade from FUJIFILM Wako Pure Chemical Corp. (Osaka, Japan). Dulbecco's modified Eagle's medium (DMEM) was purchased from Gibco Life Technologies Corporation (Grand Island, NY, USA). Penicillin-streptomycin, fetal bovine serum (FBS), and horse serum (HS) were purchased from Invitrogen-Thermo Fisher Scientific (Carlsbad, CA, USA). The Cell Count Kit-8 (WST-8) was purchased from Dojindo Laboratories (Kumamoto, Japan). The High Pure RNA Isolation Kit was purchased from Roche Applied Science (Penzberg, Germany). ReverTra Ace® qPCR RT Master Mix with gDNA Remover and KOD SYBR® qPCR Mix were purchased from Toyobo Life Science (Tokyo, Japan).

Preparation of BSA-conjugated fatty acids

CPA, TPA, and EPA (200 mM each) were conjugated with 10% fatty acid-free BSA at 4°C for 2 hr. The final concentration of BSA-conjugated CPA, TPA, and EPA was 4 mM, and they were stored at 4°C.

Cell culture

L6 myoblast cells (L6 cells) were purchased from the American Type Culture Collection (Manassas, VA, USA). The cells were maintained in DMEM containing 5 mM glucose supplemented with 10% FBS at 37°C in a humidified atmosphere containing 5% CO_2. To differentiate the myoblasts into myotubes, when the cells reached confluence (on day 2 after seeding), the medium was changed to DMEM containing 5 mM glucose (low glucose medium; LG) or 25 mM glucose (high glucose medium; HG) supplemented with 2% HS and 100 ng/ml insulin. After 2 days, the differentiation medium was replaced with fresh medium containing 2% HS and 100 ng/ml insulin. The cells were cultured for 6 days, with the medium replaced by fresh medium every 2 days, until myoblasts had fully differentiated into myotubes. In experiments aiming to examine the effect on cells during the differentiation process (days 6), CPA, TPA, and EPA (100 µM each) were added to the fresh differentiation medium used for medium replacements, and the cells were incubated for 6 days until they became fully differentiated. Thus, we divided into 5 groups (CPA (in HG), TPA (in HG), EPA (in HG), HG only, and LG only)). The cells were either harvested for RNA extraction or collected on day 6.

Cell viability assay

Cell viability was measured in a hyperglycemic environment of 25 mM glucose (in HG) with different concentrations of each fatty acid, i.e., EPA, CPA, or TPA. L6 cells were seeded at a density of 1×10^6 cells per well in 96-well plates and treated with various concentrations (100 to 400 µM) of CPA, TPA, or EPA for 3 days. Then, WST-8 was added to the wells, and the cells were incubated for 1 hr in a CO_2 incubator. The absorbance of each well was measured at 450 nm using a model 680 microplate reader (Bio-Rad Laboratories, Hercules, CA, USA).

RNA extraction and quantitative reverse transcription polymerase chain reaction PCR (RT-qPCR) for differentiation biomarkers

Total RNA was isolated from the cells using the High Pure RNA Isolation Kit according to the manufacturer's protocol [31]. The RNA quantity was determined using a GeneQuant pro RNA/DNA Calculator (Amersham Pharmacia Biotech, Cambridge, UK). Up to 2.5 µg of total RNA was used for reverse-transcription using the ReverTra Ace qPCR RT Master Mix with gDNA Remover. RT-qPCR was performed using KOD SYBR qPCR Mix (Toyobo Life Science) and a StepOne Plus Real-Time PCR System (Applied Biosystems, Foster City, CA, USA) with incubation at 98°C for 2 min followed by 40 cycles of denaturation at 98°C for 10 sec, annealing at 60°C for 10 sec, and extension at 68°C for 30 sec. Target amplification was determined by the StepOnePlus Real-Time PCR System using *β-actin* as a reference, as detailed by the manufacturer. The primer sequences used for RT-qPCR are listed in Table 1. *β-actin* was used as the normalizing gene. The significance of changes in mRNA was calculated using the 2-ΔΔt by Cq value. Repeated measurements were taken for each sample, and the experiments were performed in quadruplicate at the least. The expression level (Ct value) of *β-actin* did not differ significantly among groups.

Table 1. Primer sequences used

Gene	Forward primer (5-3)	Reverse primer (5-3)
Pax3	CAGCCCACGTCTATTCCACA	CACGAAGCTGTCGGTGTAGC
Myf5	GCTGAGGGAGCAGGTAGAGA	GACAGGGCTGTTACATTCAGG
MyoD	TGGATCAATCCCACTCTAATAGC	TTCGCTGGTAGGAAAGTGAAG
Myogenin	CTACAGGCTTGCTCA	TGGGAGTTGCATTCAC
MRF4	CCCTTACAGCTACAAACCCAAG	TGCTCCTCCTTCCTTAGCAG
Myhc2x	AAGACCGCAAGAACGTTCT	TTAAATAGAATCACATGGGGAC
Myhc2a	TCCTCAGGCTTCAAGATTTG	TTAAATAGAATCACATGGGGAC
β-actin	CCCATCTATGAGGGTTACGC	TTTAATGTCACGCACGATTTC
Tnfaip3	TGAACTTCGGGGTGATCG	GGGCTTGTCACTCGAGTTTT

Western blotting

After complete differentiation (day 6), the cells were lysed in ice-cold lysis buffer (32.9 mM Tris–HCl, pH 6.8, 22.2% glycerol, 2.2% LDS (Lithium Dodecyl Sulfate), and 0.01% bromophenol blue) with a protease inhibitor cocktail (Thermo Fisher Scientific, Tokyo, Japan). The cells were then sonicated, and collected by centrifugation at 12,500 *g* for 5 min. The protein concentration was determined using a BCA Protein Assay Kit (Takara Inc., Tokyo, Japan). Equal amounts (30 µg) of protein from each sample were loaded and separated by 10% sodium dodecyl sulfate-polyacrylamide gel electrophoresis. The proteins were then transferred to nitrocellulose membranes using a Trans-Blot SD Semi-Dry Transfer Cell (ATTO Corp., Tokyo, Japan). The membranes were blocked with fish gelatin at 25°C for 1 hr, and incubated with target primary antibodies at 4°C overnight. Monoclonal antibodies for phosphorylated Akt (p-Akt 473; #9271), pan-Akt (#9272), Phospho-p44/42 mitogen-activated protein kinase (MAPK; extracellular signal-regulated kinase (Erk) 1/2; #9106), and p44/42 MAPK (Erk1/2; #9102) were purchased from Cell Signaling Technology (Beverly, MA, USA). After being washed four times with Tris-buffered saline containing 0.1% Tween 20, the membranes were incubated with horseradish peroxidase-conjugated secondary antibodies (anti-rabbit (#7074) or anti-mouse (#7076) antibody from Cell Signaling Technology) in Tris-buffered saline with 0.1% Tween 20 for 1 hr. After being washed three times, the proteins were detected and quantified by ImageQuant LAS 4000 (GE Healthcare, Chicago, IL, USA). The protein expression level of each sample is expressed as the percentage of the relative changes to the levels of pan-Akt and p44/42 MAPK, which were used as the loading controls. The phospho-Akt and phospho-p44/42 MAPK levels were then normalized to the total pan-Akt and phospho-p44/42 MAPK levels.

Indirect immunofluorescence

When the L6 cells reached confluence (on day 2 after seeding), cells were treated with each fatty acid on a Black IsoPlate-96 TC (PerkinElmer, Waltham, MA, USA) for 4 or 6 days. Then fixed with 4% paraformaldehyde in phosphate-buffered saline (PBS) for 30 min, washed with PBS, and permeabilized with 0.5% Triton X-100 in PBS. The cells were blocked with 5% BSA in PBS for 1 hr at 25°C, then incubated with anti-myosin heavy chain mouse-mono antibody (1:500; R&D systems, MN, USA) for 1 hr, followed by incubation with Alexa 488-conjugated goat anti-mouse IgG (1:1,000; Molecular Probes, Eugene, OR, USA), rhodamine-labeled phalloidin (1:100; Molecular Probes), and DAPI (1 µM; Sigma) at 25°C for 1 hr. After being washed with PBS, Images were captured on Nicon ECLIPSE Ti inverted microscope (Nicon, Tokyo, Japan). For quantification of myosin area of anti-myosin antibody, we calculated the signal density of identically threshold adjusted fluorescent images with ImageJ system. Color image was converted into grayscale by changing it into 8-bit. Rollingball radius under substract background was needed to be changed into 50 to remove some of the background coloration from the image. All the images were measured using the same standards. Experiments were repeated on five independent occasions.

Analysis of ROS generation

Analysis of intracellular ROS generation was performed by flow cytometry. Briefly, L6 cells were plated on a µ-Slide 18 Well (ibidi GmbH, Grafelfing, Germany) at a final density of 5.0×10^4 cells/well and incubated for a day. Afterwards, cells were treated with differentiation medium or conjugated fatty acids for 6 days. Then, cells were loaded with CellROX® Green Reagent (Molecular probes, Eugene, OR, USA) and Hoechst 33342 (Bio-Rad Laboratories) for nuclear counterstaining for 30 min, fixed with 4% paraformaldehyde in PBS for 30 min, and washed with PBS. Images were acquired with a BZ-X710 fluorescent microscope (KEYENCE, Osaka, Japan) for quantification of the relative ratio nuclear and ROS signals. Experiments were repeated on five independent occasions.

Statistical analysis

All data are expressed as the mean ± standard error of the mean (SEM). The significance of differences was tested using Tukey's test and the Student's paired *t*-test. The level of significance was set at $P<0.05$ for all data analyzes.

RESULTS

Cytotoxicity of the fatty acids

We performed cytotoxicity tests to determine the suitable concentrations of CPA, TPA, and EPA to be added to cells in HG. The cytotoxic effects of CPA, TPA, and EPA at different concentrations are shown in Fig. 1b–d. After comparing the non-toxic concentrations of EPA and CPA and the half-lethal doses, it was concluded that the addition of 100 µM was appropriate, and this concentration was thus used in the following experiments.

Skeletal muscle differentiation in LG and HG

L6 myoblasts were cultured to 70% to 80% confluence, and the medium was changed to LG or HG differentiation medium. After 6 days, we analyzed the expression of mRNAs. The expression levels of *Pax3* and *Myf5* decreased by 0.8- and 0.2-fold, respectively, in cells cultured in HG when compared to those in LG (Fig. 2b and 2c). The expression levels of genes encoding skeletal muscle differentiation markers (*MyoD, Myogenin*, and *MRF4,* except *Myf5*) increased in cells cultured in HG, when compared to those in LG (Fig. 2d–f). The expression levels of *MyHC2x* and *MyHC2a* increased by 18- and 3-fold, respectively, in cells cultured in HG when compared to those in LG (Fig. 2g and 2h).

Effects of fatty acids on skeletal muscle differentiation in HG

L6 myoblasts were treated with HG medium supplemented with CPA, TPA, or EPA. The gene expression levels of *Pax3*, *Myf5*, *MyoD*, *Myogenin*, *MRF4*, *MyHC2x*, and *MyHC2a* in HG were compared between the CPA-, TPA-, and EPA-treated groups. In addition, the expression of *Tnfaip3,* which encodes the inflammatory cytokine tumor necrosis factor alpha-induced protein 3, was compared between all of the groups (LG, HG, CPA, TPA, and EPA). CPA, TPA, and EPA in HG increased the expression level of *Pax3* by 1.3-, 1.7-, and 2.0-fold, respectively, when compared to the levels of the cells in HG only. (Fig. 3a). CPA, TPA, and EPA significantly decreased the expression levels of *Myf5* and *MyoD* by 0.2-fold when compared to the levels of the cells in HG only (Fig. 3b and 3c). The expression levels of *MRF4*, *MyHC2x,* and *MyHC2a* were remarkably decreased by the treatment of each of the fatty acids (Fig. 3e–g). However, the expression level of *Myogenin* was increased by CPA treatment, and was decreased by TPA and EPA treatments when compared to the level of the cells in HG only (Fig. 3d). CPA, TPA, and EPA decreased the expression level of *Tnfaip3* by 0.6-fold after 6 days when compared to the levels of the cells in HG only (Fig. 3h).

Indirect immunofluorescence imaging

An indirect immunofluorescence method was used to examine how myosin expression changes when L6 myoblasts are exposed to HG or the treatment of each fatty acids. There was typical myotube formation at 4 and 6 days (Fig. 4a and 4b), and we evaluated the myosin area at the 6 days (Fig. 4c). After CPA, TPA, or EPA was added with HG, the area of myosin (green) was 1.5-fold higher in HG than in LG at 6 days. In contrast, CPA, TPA, or EPA treatment decreased the area of myosin by when compared to in HG, indicating that the area of myosin in treatment of each fatty acids had similar tendency to in LG.

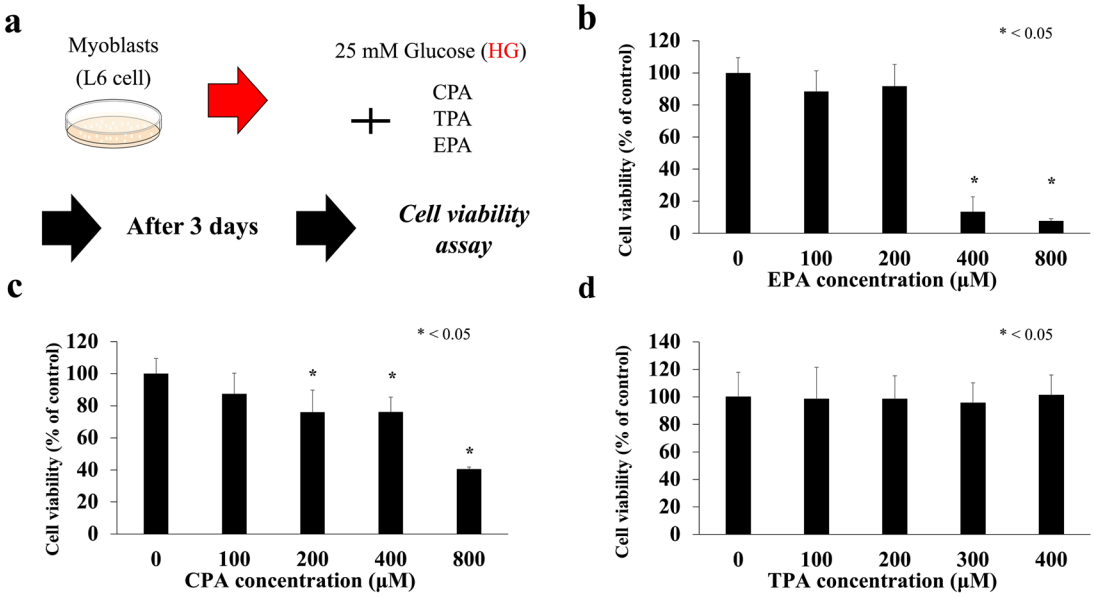

Fig. 1. Time course from cell seeding to the replacement of the high-glucose (HG) differentiation medium **(a)**. The effect of eicosapentaenoic acid (EPA: **b**), cis-palmitoleic acid (CPA: **c**) and trans-palmitoleic acid (TPA: **d**) on L6 myoblast metabolic activity by a WST-8 assay after 3 days of exposure. The bars represent the means ± SEM. Asterisks indicate $P<0.05$. n=7.

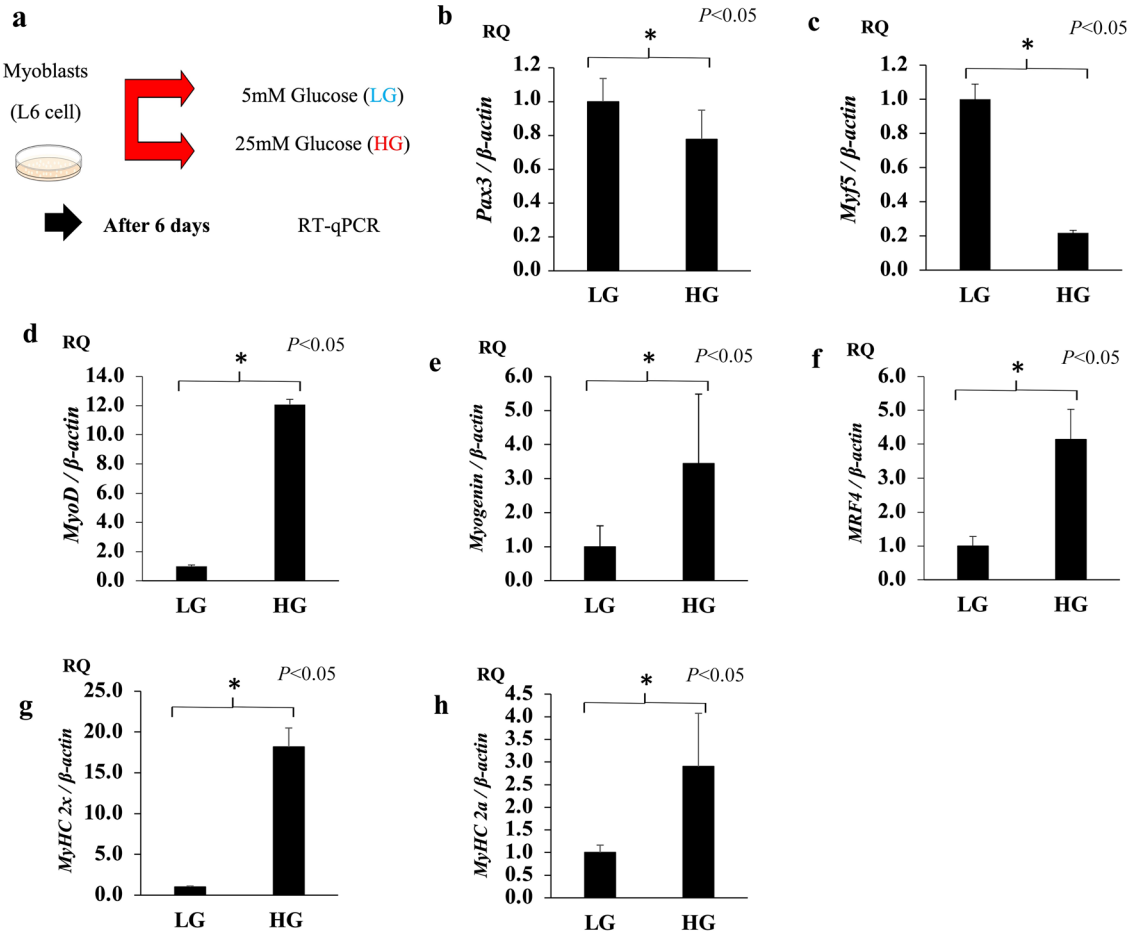

Fig. 2. Time course from cell seeding to the replacement of the differentiation medium (low glucose: LG or HG) **(a)**. The mRNA expression levels of *Pax3* **(b)**, *Myf5* **(c)** *MyoD* **(d)**, *Myogenin* **(e)**, *MRF4* **(f)**, *MyHC2x* **(g)**, and *MyHC2a* **(h)** in LG or HG. L6 myoblasts were cultured to differentiate into skeletal muscle for 6 days. The mRNA levels were determined by real-time PCR analysis and normalized to the expression level of the *β-actin* gene. The bars represent the means ± SEM. Asterisks indicate $P<0.05$. n=7.

ROS analysis

We investigated whether HG induced ROS generation, and also whether palmitoleic acids have antioxidative effects. After 6 days (Fig. 5a), ROS generation was increased by 2.8-fold in HG (Fig. 5b). TPA and EPA in HG reduced the excessive ROS generation by 0.5-fold when compared to the ROS generation level in HG only; in contrast, CPA increased ROS generation by 1.2-fold when compared to the level in HG only.

Insulin signaling in LG and HG with and without dissolved fatty acids

The metabolic and mitogenic signaling pathways were assessed by examining the phosphorylation of AKT and ERK1/2 MAP kinase, respectively. The level of phosphorylation of AKT was significantly increased by approximately 2.5-fold in HG only when compared to in LG only ($P<0.05$; Fig. 6a). Treatment with CPA increased the level of phosphorylation of AKT by approximately 2.5-fold when compared to the level in LG only (Fig. 6a). However, TPA and EPA increased the level of phosphorylation of AKT by 2-fold when compared to the level in LG only, but no significant effects were seen when compared to the level in HG only.

The level of phosphorylation of ERK1/2 was 0.4-fold lower in HG only when compared to the level in LG only (Fig. 6b). Various palmitoleic acids had different effects on MAPK/ERK signaling. TPA and EPA did not alter the level of phosphorylation of ERK1/2 when compared to the level in LG only (Fig. 6b). However, TPA and EPA increased the level of phosphorylation of ERK1/2 by approximately 3-fold when compared to the level in HG only.

DISCUSSION

We first examined the influence of a hyperglycemic environment on skeletal muscle differentiation in comparison to a hypoglycemic environment, which was predicted to reflect a normal blood glucose level. Through *in vitro* studies, we found that HG increased the gene expression of muscle regulatory factors. The myotubes that are seen in C2C12 were not seen in L6

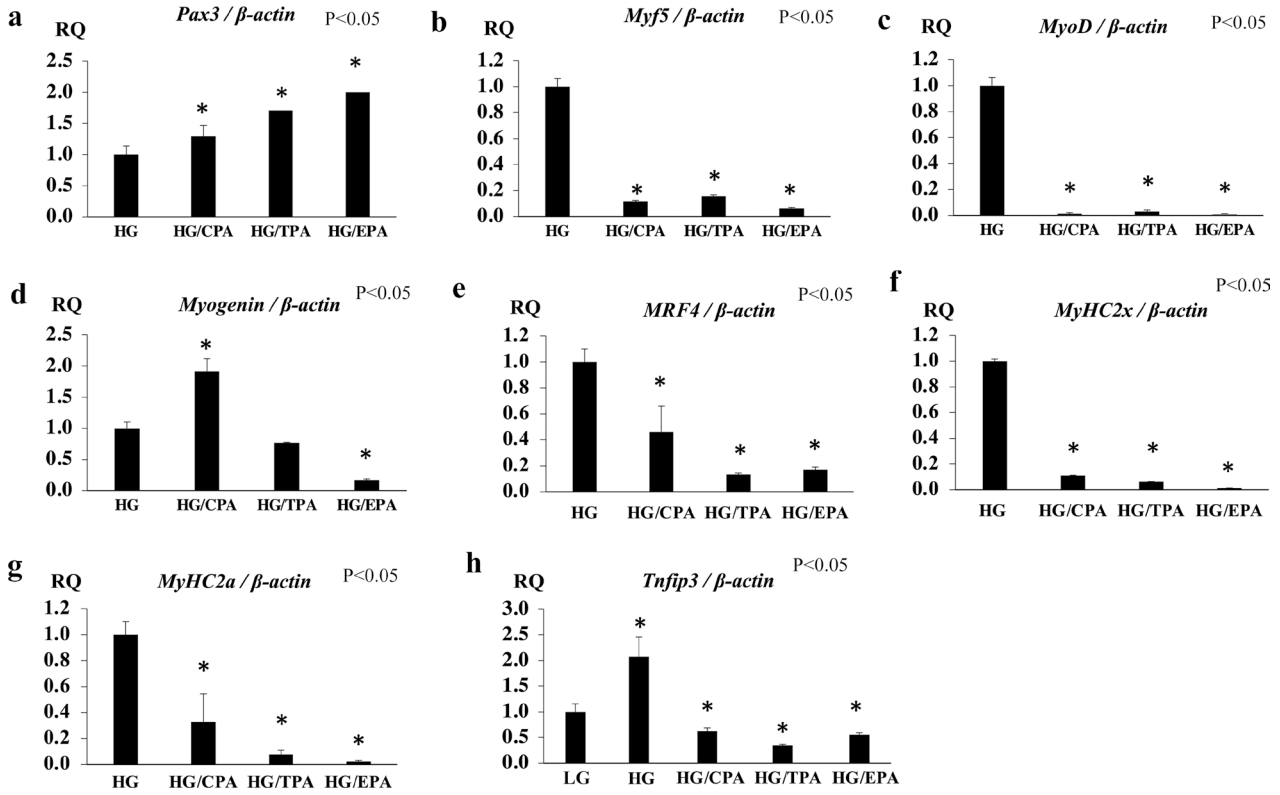

Fig. 3. The gene expression levels of *Pax3* **(a)**, *Myf5* **(b)**, *MyoD* **(c)**, *Myogenin* **(d)**, *MRF4* **(e)**, *MyHC2x* **(f)**, *MyHC2a* **(g)**, and *Tnfaip3* **(h)**. L6 cells were treated with LG only, or with CPA (100 µM; HG/CPA), TPA (100 µM; HG/TPA), or EPA (100 µM; HG/EPA) dissolved in HG for 6 days. The mRNA levels were determined by real-time PCR analysis and normalized to the expression level of the *β-actin* gene. The bars represent the means ± SEM. Tukey's HSD (honestly significant difference test). Asterisks indicate $P<0.05$ (statistical significance) when compared with the control.

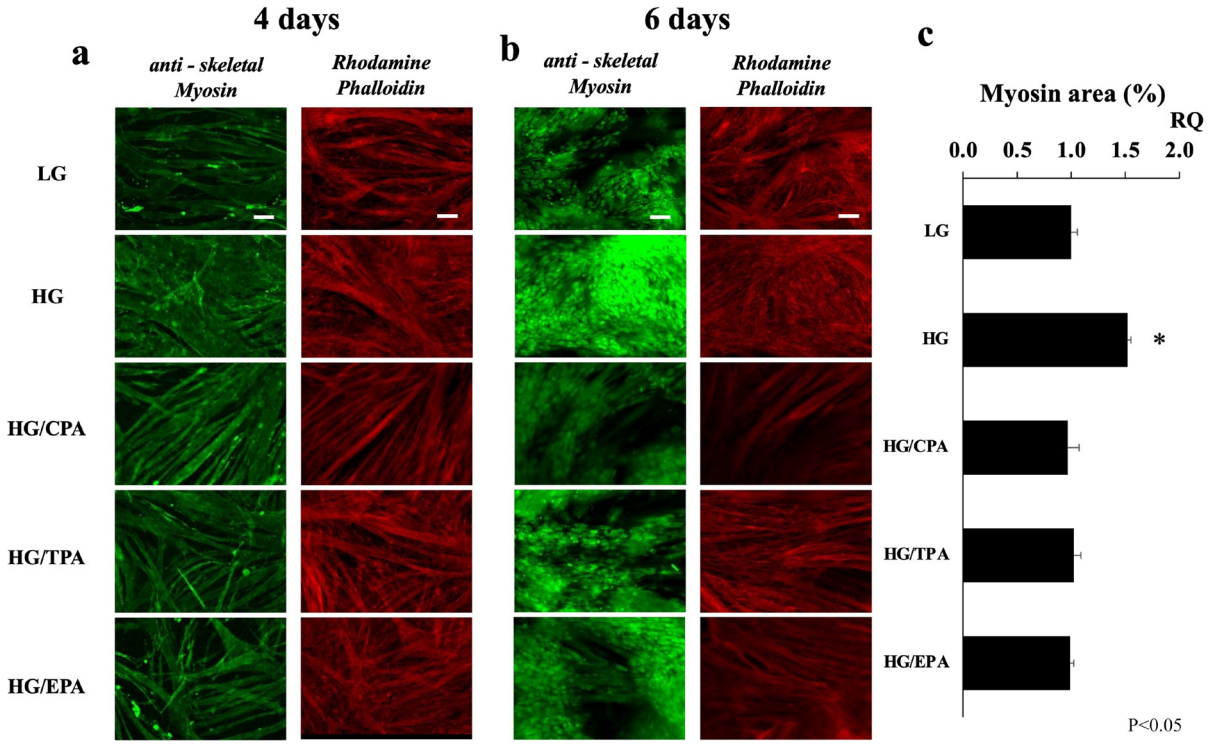

Fig. 4. Indirect immunofluorescence imaging of myosin in L6 myotubes. The effects of CPA (100 µM; HG/CPA), TPA (100 µM; HG/TPA), or EPA (100 µM; HG/EPA) in HG or LG for 4 days **(a)** and 6 days **(b)**. The cells were labeled with anti-myosin (green), rhodamine-labeled phalloidin (red) (a, b). The scale bar shows 10 µm. The quantified area of myosin on the 6 days **(c)**. The bars represent the means ± SEM. Tukey's HSD. Asterisks indicate $P<0.05$ (statistical significance) when compared with the control.

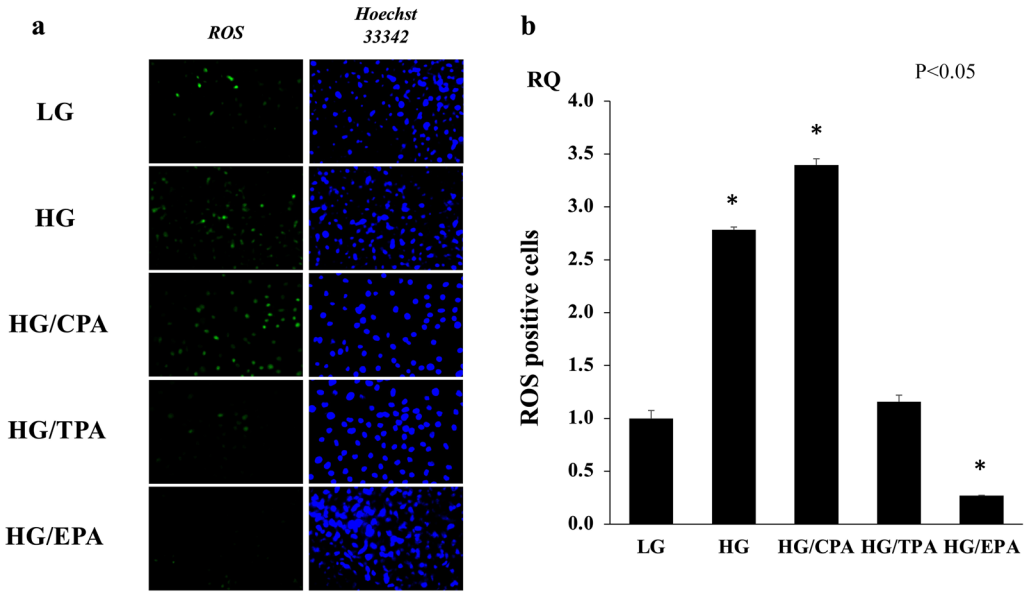

Fig. 5. The generation of ROS was analyzed using CellROX® Green Reagent (green); nuclei were counterstained with Hoechst 33342 (blue) **(a)**. The effects of CPA (100 μM; HG/CPA), TPA (100 μM; HG/TPA), or EPA (100 μM; HG/EPA) in HG or LG for 6 days were examined **(b)**. The bars represent the means ± SEM. Tukey's HSD. Asterisks indicate $P<0.05$ (statistical significance) when compared with the control.

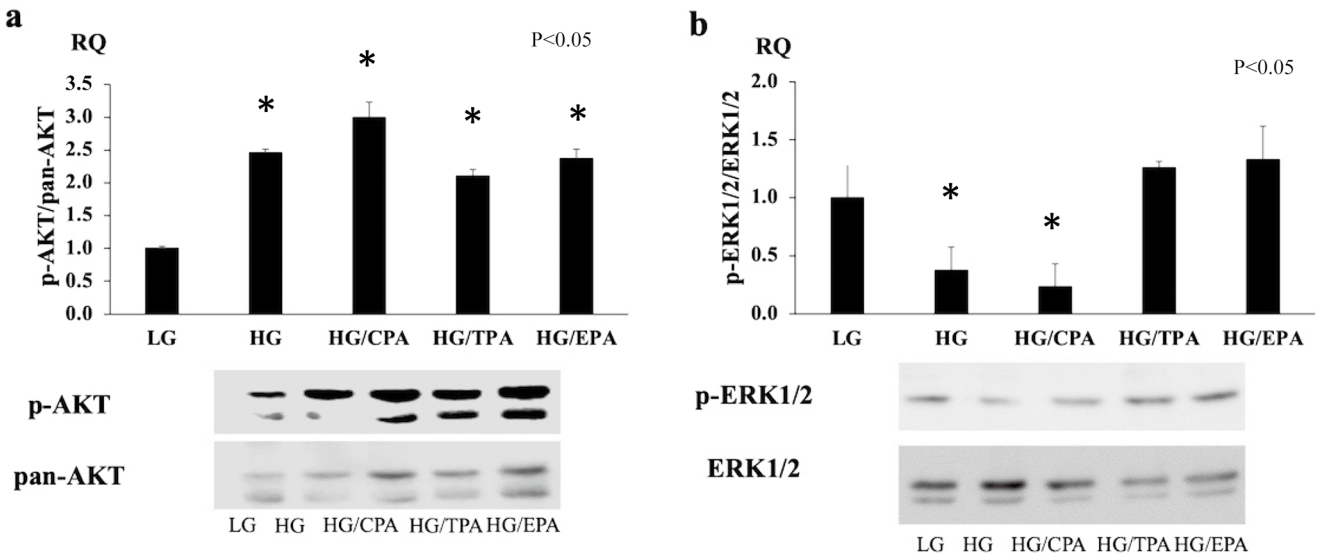

Fig. 6. Western blotting analysis of the phosphorylation levels of AKT **(a)** and ERK1/2 **(b)** in L6 myotubes. The effects of CPA (100 μM; HG/CPA), TPA (100 μM; HG/TPA), or EPA (100 μM; HG/EPA) on insulin signaling in HG for 6 days were examined. Data are shown as the means ± standard deviation of four independent experiments. Tukey's HSD. Asterisks indicate $P<0.05$ (statistical significance) when compared with the control.

cells, but HG appeared to increase the number of myosin-positive cells by enhancing differentiation. In other words, we could not reveal clear myogenic differentiation in L6 myotubes, and further studies in mouse and human myoblasts are needed. In addition, the phosphorylation of AKT and ERK1/2 are involved in signaling to promote proliferation and differentiation [16]. The skeletal muscle development process involves the IGF1-AKT-mTOR pathway, which acts as a positive regulator [28]. ERK-1/2 is required for myoblast proliferation [20]. After differentiation for 6 days, increased phosphorylation of AKT was accompanied by the promotion of differentiation via the IGF-1-AKT signal, and inhibition of the phosphorylation of ERK1/2 led to growth arrest. Furthermore, we found that HG induced ROS generation. It has been reported that hyperglycemic environments induced ROS generation [35], and another study showed that skeletal muscle differentiation induced ROS-dependent effects on *NOX4* expression. [18]. Although an increase in the level of ROS has been detected, the underlying molecular mechanism has not yet

been elucidated. It has been reported that increased production of ROS in a hyperglycemic environment can dynamically change the morphology of mitochondria [36], and lead to the overproduction of advanced glycation end products (AGEs) [1, 7], among other effects. AGEs might affect skeletal muscle function and lead to the activation of different signaling pathways mediated by several cell surface receptors [9, 26]. However, the activation of receptors for AGEs (RAGE) stimulates myogenesis, which is important for skeletal muscle development [27]. Unfortunately, it remains unclear how the activation of AGEs-RAGE signaling induces hyperglycemic environments and affects skeletal muscle differentiation. The mechanism responsible for the increased level of ROS in hyperglycemic environments is also not well understood. An increase in ROS generation in hyperglycemic environments has been reported for many cells [4, 17]. Some cell death processes that were originally thought to result from the direct toxicity of ROS have been shown to be involved in programmed and physiological cell death pathways [11, 13]. However, recent studies have suggested that a basal level of ROS is necessary for basic biological processes, such as cellular proliferation and differentiation [6, 19]. We consider that the increase in ROS generation in hyperglycemic environments influences the signals for proliferation, and promotes differentiation via inflammatory cytokines.

We also examined the proliferation and differentiation of cells in the presence of palmitoleic acids or EPA. Treatment with CPA, TPA, or EPA inhibited the expression of myosin, *Myf5*, *MyoD*, *MRF4*, *Myhc2x*, *Myhc2a* and *Tnfaip3*; this is consistent with the results of previous studies on fatty acid addition to cells [24, 37]. However, the trans and cis isomers may have different effects. The phosphorylation of AKT and inhibition of ERK1/2 are involved in L6 muscle cell differentiation and proliferation [33]. In this study, the level of phosphorylation of Akt did not decrease after the addition of TPA or EPA. In contrast, treatment with CPA promoted IGF-AKT signaling. However, it is possible that a factor other than the activation of AKT signaling promoted L6 myotube development. Moreover, analysis of the phosphorylation of ERK1/2 and ROS generation showed different influences with treatment of TPA compared to CPA. The addition of CPA led to a larger increase in ROS generation than did hyperglycemia. In contrast, TPA showed a tendency to decrease ROS generation in comparison to other fatty acids via the phosphorylation of ERK1/2. Thus, cis-palmitoleic acid did not prevent ROS generation, but exerted anti-inflammatory effects by regulating inflammatory cytokines. It has been reported that CPA decreases ROS generation and the level of inflammatory cytokines [23, 29]. Furthermore, because cis-palmitoleic acid downregulated the phosphorylation of ERK1/2, this acid may have prevented cell proliferation and differentiation by controlling the phosphorylation of ERK1/2. However, EPA and TPA were observed to have similar effects. As EPA and TPA controlled the ROS levels, and the hyperglycemic condition increased *Tnfaip3* expression, which differed from the effects observed for CPA, the anti-inflammatory action is regarded to be antioxidant action. In other words, the addition of TPA and EPA led to normal cell development, as would be observed under normoglycemic conditions. This suggests that the two structural isomers of palmitoleic acid affected skeletal muscle differentiation in a hyperglycemic environment via different mechanisms. However, the molecular mechanisms involved in the inhibition of myogenic differentiation could not be clarified. In the future, we plan to investigate the mechanism of action of cis-type and trans-type palmitoleic acids in more detail.

In this study, we found that proliferation and differentiation into myotubes promoted the increased ROS production caused by the hyperglycemic environment. When excessive hyperglycosemia persists during pregnancy, it is thought that the hyperglycemic environment promotes the growth of the fetus. The nourishment that the mother takes in is very important to promote normal development in the fetus. The growth of the fetus increases remarkably in the later stages of pregnancy, and the intake of functional fatty acids, such as EPA, can promote normal fetal growth at these stages, although there is concern about the antithrombotic activity of EPA. We believe that our research provides new insights into the excessive fetal development that occurs during hyperglycemic pregnancies as well as the possible use of functional lipids in preventing it. In the future, we would like to perform a metabolome analysis using next-generation sequencing to further examine how these functional lipids act on muscle differentiation of the offspring through signal transduction.

POTENTIAL CONFLICTS OF INTEREST. The authors have nothing to disclose.

ACKNOWLEDGMENTS. The authors thank associate professor K. Yamauchi from graduate school of agricultural and life sciences, The University of Tokyo, for his kind gift monoclonal antibody against myosin and project assistant professor T. Kurosawa, graduate school of agricultural and life sciences, The University of Tokyo, for her advice on indirect immunofluorescence experiments. This work was supported in part by JSPS KAKENHI Grants (nos. 20K11611, 15K00809 and 18K11136 to AN and RK), the grants from Dairy Products Health Science Council and Japan Dairy Association (to AN), and the Research Program of Jissen Women's University (to AN).

REFERENCES

1. Ahmad, W., Ijaz, B., Shabbiri, K., Ahmed, F. and Rehman, S. 2017. Oxidative toxicity in diabetes and Alzheimer's disease: mechanisms behind ROS/ RNS generation. *J. Biomed. Sci.* **24**: 76. [Medline] [CrossRef]
2. Baeten, J. M., Bukusi, E. A. and Lambe, M. 2001. Pregnancy complications and outcomes among overweight and obese nulliparous women. *Am. J. Public Health* **91**: 436–440. [Medline] [CrossRef]
3. Barbour, L. A., McCurdy, C. E., Hernandez, T. L., Kirwan, J. P., Catalano, P. M. and Friedman, J. E. 2007. Cellular mechanisms for insulin resistance in normal pregnancy and gestational diabetes. *Diabetes Care* **30** Suppl 2: S112–S119. [Medline] [CrossRef]
4. Busik, J. V., Mohr, S. and Grant, M. B. 2008. Hyperglycemia-induced reactive oxygen species toxicity to endothelial cells is dependent on paracrine mediators. *Diabetes* **57**: 1952–1965. [Medline] [CrossRef]
5. Catalano, P. M., Presley, L., Minium, J. and Hauguel-de Mouzon, S. 2009. Fetuses of obese mothers develop insulin resistance in utero. *Diabetes*

Care **32**: 1076–1080. [Medline] [CrossRef]
6. Clempus, R. E., Sorescu, D., Dikalova, A. E., Pounkova, L., Jo, P., Sorescu, G. P., Schmidt, H. H., Lassègue, B. and Griendling, K. K. 2007. Nox4 is required for maintenance of the differentiated vascular smooth muscle cell phenotype. *Arterioscler. Thromb. Vasc. Biol.* **27**: 42–48. [Medline] [CrossRef]
7. Coughlan, M. T., Thorburn, D. R., Penfold, S. A., Laskowski, A., Harcourt, B. E., Sourris, K. C., Tan, A. L., Fukami, K., Thallas-Bonke, V., Nawroth, P. P., Brownlee, M., Bierhaus, A., Cooper, M. E. and Forbes, J. M. 2009. RAGE-induced cytosolic ROS promote mitochondrial superoxide generation in diabetes. *J. Am. Soc. Nephrol.* **20**: 742–752. [Medline] [CrossRef]
8. Duggleby, S. L. and Jackson, A. A. 2002. Higher weight at birth is related to decreased maternal amino acid oxidation during pregnancy. *Am. J. Clin. Nutr.* **76**: 852–857. [Medline] [CrossRef]
9. Egawa, T., Tsuda, S., Goto, A., Ohno, Y., Yokoyama, S., Goto, K. and Hayashi, T. 2017. Potential involvement of dietary advanced glycation end products in impairment of skeletal muscle growth and muscle contractile function in mice. *Br. J. Nutr.* **117**: 21–29. [Medline] [CrossRef]
10. Ehrenberg, H. M., Mercer, B. M. and Catalano, P. M. 2004. The influence of obesity and diabetes on the prevalence of macrosomia. *Am. J. Obstet. Gynecol.* **191**: 964–968. [Medline] [CrossRef]
11. Fulda, S., Gorman, A. M., Hori, O. and Samali, A. 2010. Cellular stress responses: cell survival and cell death. *Int. J. Cell Biol.* **2010**: 214074. [Medline] [CrossRef]
12. Innis, S. M. 2007. Dietary (n-3) fatty acids and brain development. *J. Nutr.* **137**: 855–859. [Medline] [CrossRef]
13. Jacobson, M. D. 1996. Reactive oxygen species and programmed cell death. *Trends Biochem. Sci.* **21**: 83–86. [Medline] [CrossRef]
14. Jones, M. L., Mark, P. J., Mori, T. A., Keelan, J. A. and Waddell, B. J. 2013. Maternal dietary omega-3 fatty acid supplementation reduces placental oxidative stress and increases fetal and placental growth in the rat. *Biol. Reprod.* **88**: 37. [Medline] [CrossRef]
15. Kalupahana, N. S., Claycombe, K., Newman, S. J., Stewart, T., Siriwardhana, N., Matthan, N., Lichtenstein, A. H. and Moustaid-Moussa, N. 2010. Eicosapentaenoic acid prevents and reverses insulin resistance in high-fat diet-induced obese mice via modulation of adipose tissue inflammation. *J. Nutr.* **140**: 1915–1922. [Medline] [CrossRef]
16. Li, J. and Johnson, S. E. 2006. ERK2 is required for efficient terminal differentiation of skeletal myoblasts. *Biochem. Biophys. Res. Commun.* **345**: 1425–1433. [Medline] [CrossRef]
17. Lin, Y., Berg, A. H., Iyengar, P., Lam, T. K., Giacca, A., Combs, T. P., Rajala, M. W., Du, X., Rollman, B., Li, W., Hawkins, M., Barzilai, N., Rhodes, C. J., Fantus, I. G., Brownlee, M. and Scherer, P. E. 2005. The hyperglycemia-induced inflammatory response in adipocytes: the role of reactive oxygen species. *J. Biol. Chem.* **280**: 4617–4626. [Medline] [CrossRef]
18. Liu, X., Heras, G., Lauschke, V. M., Mi, J., Tian, G. and Gastaldello, S. 2020. High glucose-induced oxidative stress accelerates myogenesis by altering SUMO reactions. *Exp. Cell Res.* **395**: 112234. [Medline] [CrossRef]
19. Mittler, R. 2017. ROS Are good. *Trends Plant Sci.* **22**: 11–19. [Medline] [CrossRef]
20. Mozaffarian, D., Cao, H., King, I. B., Lemaitre, R. N., Song, X., Siscovick, D. S. and Hotamisligil, G. S. 2010. Trans-palmitoleic acid, metabolic risk factors, and new-onset diabetes in U.S. adults: a cohort study. *Ann. Intern. Med.* **153**: 790–799. [Medline] [CrossRef]
21. Myatt, L. and Cui, X. 2004. Oxidative stress in the placenta. *Histochem. Cell Biol.* **122**: 369–382. [Medline] [CrossRef]
22. Ndubueze, C. O., Larraine, H. P., Saeid, B. A., Satish, K. and Patrick, M. C. 2004. Longitudinal changes in energy expenditure and body composition in obese women with normal and impaired glucose tolerance. *Am. J. Physiol.* **287**: 472–579.
23. Nisr, R. B., Shah, D. S. and Hundal, H. S. 2020. Mono- and polyunsaturated Fatty acids counter palmitate-Induced mitochondrial dysfunction in rat skeletal muscle cells. *Cell. Physiol. Biochem.* **54**: 975–993. [Medline] [CrossRef]
24. Pahlavani, M., Wijayatunga, N. N., Kalupahana, N. S., Ramalingam, L., Gunaratne, P. H., Coarfa, C., Rajapakshe, K., Kottapalli, P. and Moustaid-Moussa, N. 2018. Transcriptomic and microRNA analyses of gene networks regulated by eicosapentaenoic acid in brown adipose tissue of diet-induced obese mice. *Biochim. Biophys. Acta Mol. Cell Biol. Lipids* **1863**: 1523–1531. [Medline] [CrossRef]
25. Pérez-Matute, P., Pérez-Echarri, N., Martínez, J. A., Marti, A. and Moreno-Aliaga, M. J. 2007. Eicosapentaenoic acid actions on adiposity and insulin resistance in control and high-fat-fed rats: role of apoptosis, adiponectin and tumour necrosis factor-α. *Br. J. Nutr.* **97**: 389–398. [Medline] [CrossRef]
26. Ramasamy, R., Yan, S. F. and Schmidt, A. M. 2011. Receptor for AGE (RAGE): signaling mechanisms in the pathogenesis of diabetes and its complications. *Ann. N. Y. Acad. Sci.* **1243**: 88–102. [Medline] [CrossRef]
27. Riuzzi, F., Sorci, G., Sagheddu, R., Chiappalupi, S., Salvadori, L. and Donato, R. 2018. RAGE in the pathophysiology of skeletal muscle. *J. Cachexia Sarcopenia Muscle* **9**: 1213–1234. [Medline] [CrossRef]
28. Schiaffino, S., Dyar, K. A., Ciciliot, S., Blaauw, B. and Sandri, M. 2013. Mechanisms regulating skeletal muscle growth and atrophy. *FEBS J.* **280**: 4294–4314. [Medline] [CrossRef]
29. Souza, C. O., Valenzuela, C. A., Baker, E. J., Miles, E. A., Rosa Neto, J. C. and Calder, P. C. 2018. Palmitoleic acid has stronger anti-Inflammatory potential in human endothelial cells compared to oleic and palmitic acids. *Mol. Nutr. Food Res.* **62**: e1800322. [Medline] [CrossRef]
30. Vera, F. E., Miyazaki, H., Takahashi, K., Hara, K. and Matsuura, H. 2018. Initial studies on isolation and characterization of antioxidant compounds from immature berries of ampelopsis grandulosa, pp. 17–19., 13th Paris Int'l Conference on Chemical, Agriculture, Biological & Environmental Sciences (PABEMS-18), Paris.
31. von Schacky, C. 2020. Omega-3 fatty acids in pregnancy-the case for a target omega-3 Index. *Nutrients* **12**: 1–12. [Medline] [CrossRef]
32. Yan, X., Huang, Y., Zhao, J. X., Long, N. M., Uthlaut, A. B., Zhu, M. J., Ford, S. P., Nathanielsz, P. W. and Du, M. 2011. Maternal obesity-impaired insulin signaling in sheep and induced lipid accumulation and fibrosis in skeletal muscle of offspring. *Biol. Reprod.* **85**: 172–178. [Medline] [CrossRef]
33. Yang, H., Li, F., Kong, X., Yuan, X., Wang, W., Huang, R., Li, T., Geng, M., Wu, G. and Yin, Y. 2012. Chemerin regulates proliferation and differentiation of myoblast cells via ERK1/2 and mTOR signaling pathways. *Cytokine* **60**: 646–652. [Medline] [CrossRef]
34. Yogev, Y. and Langer, O. 2008. Pregnancy outcome in obese and morbidly obese gestational diabetic women. *Eur. J. Obstet. Gynecol. Reprod. Biol.* **137**: 21–26. [Medline] [CrossRef]
35. Youm, T. H., Woo, S. H., Kwon, E. S. and Park, S. S. 2019. NADPH oxidase 4 contributes to myoblast fusion and skeletal muscle regeneration. *Oxid. Med. Cell. Longev.* **2019**: 3585390. [Medline] [CrossRef]
36. Yu, T., Robotham, J. L. and Yoon, Y. 2006. Increased production of reactive oxygen species in hyperglycemic conditions requires dynamic change of mitochondrial morphology. *Proc. Natl. Acad. Sci. USA* **103**: 2653–2658. [Medline] [CrossRef]
37. Zhang, J., Xu, X., Liu, Y., Zhang, L., Odle, J., Lin, X., Zhu, H., Wang, X. and Liu, Y. 2019. EPA and DHA Inhibit myogenesis and downregulate the expression of muscle-related genes in C2C12 myoblasts. *Genes (Basel)* **10**: 1–13. [Medline]